SPE 62935

Use of Solvents To Improve the Productivity of Gas Condensate Wells

Liangui Du, Jacob G. Walker, SPE, Gary A. Pope, SPE, Mukul M. Sharma, SPE, Peng Wang, SPE, Center for Petroleum and Geosystems Engineering, The University of Texas at Austin

This paper was prepared for presentation at the 2000 SPE Annual Technical Conference and Exhibition held in Dallas, Texas, 1–4 October 2000.

Abstract

Experiments have been done with a retrograde gas condensate fluid to measure the decrease in gas relative permeability due to liquid dropout below the dew point and to evaluate the use of methanol to restore the gas relative permeability. The methanol was found to increase the end-point gas relative permeability by a factor of 1.2 to 2.5 depending on the initial water saturation. A likely reason for the increased gas permeability is the miscible displacement of the condensate and water phases by the methanol. The use of an inexpensive solvent such as methanol to improve the productivity of gas wells that have been damaged by production below the dew point due to condensate and/or water blocking presents an attractive approach deserving further investigation.

Introduction

In gas condensate reservoirs, when the bottom hole pressure in flowing wells falls below the dew point of the fluid a liquid hydrocarbon phase is formed. This retrograde condensate formation results in buildup of a liquid phase around the wellbore leading to a decrease in the effective permeability to gas into the wellbore. The productivity loss associated with condensate buildup can be substantial. In several instances well productivities have been reported to decline by a factor of 2 to 4 as a result of condensate accumulation.[1,2]

It has long been recognized that the formation of condensate in the vicinity of the wellbore can occur much before the average reservoir pressure falls below the dew point. Afidick *et al.*[1] and Barnum *et al.*[2] have reported case studies that show that under some conditions a significant loss in well productivity can occur due to near-wellbore condensate accumulation. Boom *et al.*[3] have pointed out that even for lean gas, with very low condensate dropout, relatively high condensate saturations can build up in the near-wellbore region as large volumes of gas flow to the well.

Since the reduction in well productivity is primarily associated with the reduction in gas relative permeability, there has been a great deal of effort put into understanding the effect of condensate dropout on gas relative permeability. Boom *et al.*,[4] Asar and Handy,[5] Hartman and Cullick,[6] and Henderson *et al.*,[7] among others, have conducted experiments to measure the gas relative permeability as a function of condensate saturation and interfacial tension. A model for predicting gas relative permeabilities as a function of gas saturation and trapping number (a generalization of the capillary and Bond numbers) was developed by Pope *et al.*[8] This model includes the dependence of gas relative permeability on interfacial tension, pressure gradient and buoyancy forces. Narayanaswamy *et al.*[9] showed that the condensate saturation and gas relative permeability near the wellbore are a strong function of the trapping number. In general, regions of high trapping numbers such as high permeability layers with high flow rates near the well show lower condensate saturations and, therefore, higher gas relative permeabilities.

The effects of condensate dropout on gas relative permeability are closely coupled with non-Darcy effects that can be significant in high rate wells.[10,11] Narayanaswamy *et al.*[12] have shown that reservoir heterogeneity plays an important role in determining the effective β (non-Darcy flow coefficient) for gas inflow into high rate gas wells. The additional pressure drop resulting from non-Darcy flow effects are closely coupled with the pressure profile and, therefore, the phase behavior in the near wellbore region.

The primary strategy for stimulating wells that show large skins due to condensate dropout has been hydraulic fracturing. In many wells it is possible to reduce the drawdowns, i.e., increase the flowing bottom hole pressure by inducing a hydraulic fracture that significantly increases the area available for inflow. This allows the well to be produced at higher bottom hole pressures for longer periods of time thereby delaying the onset of condensate formation around the wellbore. Kumar[13] has recently simulated the performance of fractured gas condensate wells and the impact of phase behavior on the performance of such fractured gas producers. However, in many instances it is not possible to induce hydraulic fractures in gas condensate wells because of complications such as the presence of a water zone or due to cost considerations. For this reason, alternative strategies have been sought for the stimulation of such gas condensate wells.

In this paper, we propose the use of alcohols to stimulate production from gas condensate wells that show a substantial reduction in productivity due to near wellbore condensate buildup or water blocking or the combined effect of high condensate and water saturations. We present for the first time experimental data that shows significant enhancement in gas relative permeabilities as methanol is injected into cores that have been damaged by the presence of a liquid condensate phase. We believe that this strategy has significant potential for improving the productivity of wells impaired by a condensate blocking mechanism at a fraction of the cost associated with drilling new wells or hydraulic fracturing even when feasible.

Experimental Apparatus and Procedures

Gas Mixture Properties. A hydrocarbon mixture of methane (C1), n-butane (C4), n-heptane (C7) and n-decane (C10) was used in all experiments. The composition of this mixture is shown in Table 2. The PVT properties of the gas mixture were measured with a windowed PVT cell using a constant composition expansion process. The gas mixture was transferred into the PVT cell at 3000 psig. The dew point of the mixture and the liquid dropout data were measured at 145°F. Figure 1 shows the phase envelop for the gas mixture calculated using the Peng-Robinson equation-of-state (PREOS). The conditions for the coreflood experiments were chosen in the retrograde condensate region at a temperature of 145°F. The measured liquid dropout is shown in Fig. 2. The liquid dropout calculated using the PREOS is also shown for comparison with the data.

The viscosity of the flowing gas phase was measured using a capillary tube viscometer. The capillary tube is placed at the end of the core holder in parallel with the effluent flow line. The pressure drop across the capillary tube was measured and Poiseuille's law was used to calculate viscosity. The viscosity of pure methane was used to calibrate the measurements.

Interfacial Tension Measurements. Interfacial tensions between the liquid and gas hydrocarbon phases were measured using a high temperature, high pressure, spinning drop tensiometer. Figure 3 shows the interfacial tension as a function of pressure at 145°F. The measured values agree well with those calculated using a parachor correlation and the PREOS. The coreflooding apparatus is shown in Fig. 4. A core holder in the vertical position with multiple pressure ports was used to measure pressure drop across four sections of the core. The permeability and relative permeability during all displacements were calculated from these pressure data. Each section of the core is approximately two inches long. Back-pressure regulators were used at both the upstream and downstream ends of the core to allow the fluid to be flashed at the upstream end of the core to provide a steady state flow of gas and condensate at some desired pressure below the dew point pressure. The entire apparatus is placed in a temperature-controlled oven at 145°F.

Core Preparation. Texas Cream limestone cores were cut from a single block of limestone. Permeability measurements reported here clearly show that the cores are nearly homogeneous with a porosity of 0.20 and permeabilities varying from 4 to 11 md. The cores were wrapped in aluminum foil and shrink tubing applied to eliminate the diffusion of gases through the Viton sleeve.

The initial water saturation was established by a procedure that was designed to achieve relatively low and uniform water saturation representative of many gas condensate reservoirs. The core was initially saturated with water containing 0.05 weight percent calcium chloride. It was then dried in an oven at 220°F for at least 24 hours to remove all of the water, placed in the core holder, evacuated for 24 hours and exposed to water vapor by a series of push-pull cycles using a hand pump. This procedure of allowing water vapor to come into contact with the core through a series of push and pull cycles, allowed us to establish a nearly uniform water saturation throughout the core with a water containing 0.5 wt.% calcium chloride. Steady state gas pressure drop data measured for each section of each core showed that the gas permeability was uniform along the length of each core, which allows us to infer that the water saturation was nearly uniform as well. In most cases, this procedure required between 20 and 40 push-pull cycles. The water saturation was determined gravimetically.

Core Flooding Procedures. A new method was used in this study to obtain the gas relative permeability after condensate dropout. The single-phase gas permeability was first measured by setting the outlet back-pressure regulator to 3000 psig and injecting a single-phase gas mixture into the core at constant rate using a Ruska pump until steady state was reached. This same mixture at 3000 psig was then injected at a constant rate into the upstream back-pressure regulator set at 3000 psig and with the outlet back-pressure regulator set at a pressure below the dew point pressure (e.g. 1200 psig). This was done so that the high pressure gas mixture would flash into a two-phase mixture of gas and condensate as it flowed into the core. This procedure mimics the dynamic accumulation of condensate around the wellbore as the bottom hole pressure drops below the dew point. The condensate injected into the core accumulates with time and reduces the relative permeability to gas. The gas and condensate reach a steady state fractional flow that depends on the relative permeability characteristics of the core at the given connate water saturation. Figure 5 illustrates the typical pressure response observed at different ports along the length of the core as this process of condensate accumulation occurs. It is quite evident that the accumulation of condensate proceeds sequentially from the inlet of the core to the outlet. The produced fluids are collected in a windowed cell connected to the downstream back-pressure regulator. The condensate saturation was calculated by measuring the volumes of gas injected and the volumes of gas and liquid produced in the windowed cell. The relative permeability of the gas and condensate was then calculated from the steady state pressure drops across each section of the core.

Next gas in equilibrium with the condensate at the outlet pressure of the core was injected into the core to measure the end-point gas relative permeability in the presence of residual water and condensate. Then liquid methanol was injected into the core and the pressure drop across different sections of the core measured as a function of time. Methanol is a solvent that is miscible with both liquid water and liquid condensate under these conditions. The condensate accumulation step was then repeated at the same pressure (usually 1200 psig) and the gas and condensate relative permeabilities once again measured followed by the equilibrium gas end-point relative permeability measurement at steady state and the same pressure. To study the extent and the duration over which the gas relative permeability is increased due to the methanol injection, several tens of pore volumes of gas were injected into the core during the final step of each coreflood.

Experimental Results and Discussion

Table 1 lists the important properties of the Texas Cream limestone cores used in all our experiments. Table 2 lists the composition of the gas condensate fluid used. Table 3 shows the gas viscosity measured using the capillary viscometer. The interfacial tensions between the gas and the condensate phases measured using the spinning drop tensiometer are shown in Fig. 3.

Figure 5 shows an example of a typical plot of the pressure drop across the four sections of the core as condensate accumulation occurs within the core. In the section closest to the inlet (section 1), the pressure drop increases from about 1 psi to about 6 psi, indicating a reduction in gas permeability by a factor of about 18 (since the gas viscosity is approximately 3 times lower at 1200 psig compared to 3000 psig). Table 4 shows the gas relative permeability for two-phase flow at the end of condensate accumulation for the entire core. Very low values on the order of 0.01 were observed. For example, the steady state gas relative permeability for experiment 8 at 1200 psig was 0.027 for two-phase flow compared to 0.22 for single-phase flow of gas at residual condensate saturation and 20% water saturation.

As the condensate reaches sections 2, 3 and 4, the respective pressure drops increase by about the same ratio. This may be the first time an experimental observation of the dynamics of condensate buildup in a coreflood experiment has been reported in the literature. Approximately six pore volumes of gas and condensate were injected into the core to achieve a steady state flow with a condensate fractional flow of 0.16 and a condensate saturation of about 0.44. Fewer pore volumes were required to reach steady state at higher water saturations since the volume of condensate accumulated is not as high. Also, fewer pore volumes were required to reach steady state at 2500 psig compared to 1200 psig since the liquid dropout is higher at 2500 psig.

After steady state condensate buildup, equilibrium gas was injected into the core until residual condensate saturation was reached. Residual condensate saturations based on the volume of condensate produced are listed in Table 5. For experiment 6, the residual condensate saturation was 34%. The residual condensate saturation depends on the water saturation and the capillary number. In general higher capillary numbers and lower water saturations lead to lower residual condensate saturations.

Figure 6 shows the pressure drop across the core for experiment 7 before methanol and after methanol injection. The use of methanol results in a significantly lower pressure drop and thus a significantly higher gas end-point relative permeability. Note that the pressure drop across the core for the gas flood after methanol is still slowly decreasing after 14 pore volumes when the experiment was stopped. Figure 7 shows the increase in end-point gas relative permeability due to methanol injection for several corefloods at different initial water saturations. The increase in the gas permeability varies from a factor of 1.2 to 2.5 for these corefloods depending on the initial water saturation. Higher initial water saturation results in a larger increase in gas relative permeability after methanol treatment, which indicates that it is the combined effect of condensate and water that reduces the gas permeability. The initial water saturation was made much higher in Experiment 12 in part to test this interpretation. Unlike all of the other experiments, water was injected and then displaced by gas to a residual value rather than established by the condensate procedure. This resulted in a much higher and less uniform value of water saturation with the overall average in all 4 sections of the core equal to 50%. This resulted in a steady state two-phase flow condensate saturation of 8% and a gas relative permeability of only 0.007.

Table 6 shows the end-point gas relative permeabilities for the different sections of the core before and after methanol treatment. Each section shows an increase in gas permeability. There is no clear trend showing a disproportionate increase in permeability for any of the sections, which indicates that the observed increase in gas permeability is not due to experimental artifacts such as the elimination of capillary end effect. Such effects are small in our experiments.

Figure 8 shows the relative permeability as a function of capillary number at gas saturations over three different ranges. It is clearly seen that the gas relative permeability increases with capillary number for a given gas saturation. This is consistent with the models presented by Pope, *et al.*[8] Figure 9 shows similar results for gas relative permeability for three different ranges of capillary number. Again, the same trends are observed. There is considerable scatter in the data due to differences in the conditions between experiments. However, it is interesting to note that both two-phase and three-phase data seem to follow the same general trends. This suggests that the end-point gas relative permeability to a first order is sensitive only to the gas saturation and the capillary number and not to the saturations of water and condensate separately.

To explore the underlying reasons behind the increase in gas relative permeability due to methanol injection, two hypotheses were investigated. The first possibility is that the methanol causes a decrease in the interfacial tension (IFT) between the gas and condensate phases resulting in larger capillary numbers and low residual condensate saturations. To investigate this possibility, interfacial tension measurements were conducted under temperature and pressure conditions of the coreflood experiments using a spinning drop tensiometer. The data obtained with mixtures of methanol and hydrocarbons are presented in Fig. 10 and compared to the values computed from the parachors and the PREOS. A condensate liquid with composition C1=0.34, C4=0.40, C7=0.19, C10=0.07 was mixed with methanol and then a gas bubble formed to measure these IFT data. The methanol increased the IFT, so IFT reduction is not likely to be the explanation for the increase in gas permeability.

The second possible explanation for the increase in gas permeability by methanol injection is a change in the phase behavior resulting from the methanol mixed with the water and condensate. To explore this possibility further, phase behavior studies using this same hydrocarbon composition were conducted with mixtures of methanol and the hydrocarbons. Figure 11 shows that the bubble point pressure decreases with increasing mole fractions of methanol. Note that mixtures of the hydrocarbons and methanol are miscible at 1200 psig and form at most two phases (a gas and a methanol-rich liquid) when the pressure drops below the bubble point.

Figure 12 shows how the volumes of the phases change with the overall mole fraction of the methanol when a hydrocarbon mixture with composition of C1=0.62, C2=0.24, C7=0.10 and C10=0.035 is taken at 1200 psig and mixed with methanol and brine. In the absence of brine, only a single liquid phase is observed. This is because the methanol is miscible with the condensate phase in all proportions at this pressure and temperature. Addition of 0.5 wt.% $CaCl_2$ brine results in the formation of a second liquid phase. In the absence of methanol, this would correspond to an aqueous phase and a condensate phase. However, since methanol partitions into both the aqueous and condensate phases the proportion of each phase changes with the mole fraction of methanol.

The picture that emerges from our phase behavior studies is one in which the methanol displaces the aqueous and condensate phases leaving behind a methanol-rich phase in contact with the flowing gas phase. Subsequent injection of the hydrocarbon gas mixture does not result in the formation of a third condensate phase because of the presence of methanol in the pore space. As the methanol phase is gradually vaporized into the flowing gas stream, the relative permeability to gas increases further. The effect is persistent since the methanol will slowly partition into the gas phase over time. Once the methanol is completely exhausted, the condensate phase will again begin to form and build up and the gas permeability will likely decrease again. However, since the water has been completely removed from the core, the relative permeability to gas, even in the presence of condensate, may be higher. Additional experiments need to be conducted to completely study the effects of two-phase verses three-phase flow with methanol. Our experimental data suggest that the removal of the water and condensate phases produces a significant increase in the end-point gas relative permeability.

Conclusions

Based on the experiments conducted in this study, the following conclusions can be made:

1. The injection of methanol into cores in which the gas relative permeability has been reduced due to the presence of a condensate phase, can substantially improve the gas relative permeability.
2. A likely reason for the increased gas permeability is the miscible displacement of the condensate and water phases by the methanol. Condensate buildup may not begin until most of the methanol has been stripped from the pore space. Even when this buildup does occur, the effective permeability to gas may be higher since the water has been removed from the pore space.
3. The beneficial effects of methanol injection are more pronounced at higher initial water saturations since it is the combined effect of condensate and water blocking that reduces the gas permeability.
4. A new method of condensate buildup in laboratory coreflooding experiments has been presented. This method more closely corresponds to condensate buildup in the near-wellbore region of gas condensate reservoirs than convention coreflooding methods.
5. Increases in end-point gas relative permeabilities with capillary number and gas saturation were clearly observed both in our two-phase and three-phase steady state corefloods. The total liquid saturation would appear to be the most important variable causing low gas permeability.
6. The use of methanol and potentially other alcohols as solvents may provide under some conditions a less expensive method for the improvement of gas condensate well productivity than alternatives such as hydraulic fracturing.

Additional work needs to be done to study the phase behavior of hydrocarbon-water-alcohol mixtures that may be used under different reservoir conditions, in particular, at higher temperatures.

Acknowledgments

We would like to acknowledge the financial support provided by Mobil, Texaco, Saudi Aramco and JNOC for this research. We would also like to acknowledge the assistance of Bruce Rouse for his valuable help with the experiments, Jim Dixon for valuable suggestions on how to establish uniform water saturation in the cores, and Rajeev Kumar for his help with the EOS and IFT calculations.

Nomenclature

k = Permeability
k_{rg} = Relative permeability of gas phase
k^{o}_{rg} = Endpoint relative permeability of gas phase
N_c = Capillary number
P = Pressure
PV = Pore volume(s)
Q = Flow rate
S_w = Water saturation
S_o = Oil (condensate) saturation
S_{or} = Residual oil saturation
wt = Weight percent

References

1. Afidick, D., N. J. Kaczorowski and S. Bette: "Production Performance of a Retrograde Gas: A Case Study of the Arun Field," paper SPE 28749 presented at the 1994 Asia Pacific Oil & Gas Conference, Melbourne, Australia, Nov. 7-10.
2. Barnum, R. S., F. P. Brinkman, T. W. Richardson and A. G. Spillette: "Gas Condensate Reservoir Behavior: Productivity and Recovery Reduction Due to Condensation," paper SPE 30767 presented at the 1995 SPE Annual Technical Conference & Exhibition, Dallas, Texas, Oct. 22-25.
3. Boom, W., K. Wit, J. P. W. Zeelenberg, H. C. Weeda and J. G. Maas: "On the Use of Model Experiments for Assessing Improved Gas-Condensate Mobility Under Near-Wellbore Flow Conditions," paper SPE 36714 presented at the 1996 SPE Annual Technical Conference and Exhibition, Denver, Colorado, Oct. 6-9.
4. Boom, W., K. Wit, A. M. Schulte, S. Oedai, J. P. W. Zeelenberg and J. G. Maas: "Experimental Evidence for Improved Condensate Mobility at Near-wellbore Flow Conditions," paper SPE 30766 presented at the 1995 SPE Annual Technical Conference and Exhibition, Dallas, Texas, Oct. 22-25.
5. Asar, H. and L. L. Handy: "Influence of Interfacial Tension on Gas/Oil Relative Permeability in a Gas-Condensate System," *SPERE* (Feb. 1988) 257-264.
6. Hartman, K. J. and A. S. Cullick: "Oil Recovery by Gas Displacement at Low Interfacial Tension," *J. Pet. Sci. and Eng.* (1994) **10**, 197-210.
7. Henderson, G. D., A. Danesh, D. H. Tehrani, S. Al-Shaidi and J. M. Peden: "Measurement and Correlation of Gas Condensate Relative Permeability by the Steady-State Method," *SPE Res. Eval. & Eng.* (April 1998) **1**(2) 134.
8. Pope, G. A., W. Wu, G. Narayanaswamy, M. Delshad, M. M. Sharma and P. Wang: "Modeling Relative Permeability Effects in Gas-Condensate Reservoirs with a New Trapping Model," *SPE Res. Eval. & Eng.* (April, 2000) **3**(2) 171.
9. Narayanaswamy, G., G. A. Pope and M. M. Sharma: "Predicting Gas-Condensate Well Productivity Using Capillary Number and Non-Darcy Effects," paper SPE 51910 presented at the 1999 SPE Reservoir Simulation Symposium, Houston, TX, 14-17 February.
10. Wang, X. and K. K. Mohanty: "Multiphase Non-Darcy Flow in Gas Condensate Reservoirs," SPE 56486 presented at the 1999 SPE Annual Technical Conference and Exhibition held in Houston, Texas, Oct. 3-6.
11. Coles, M. E. and K. J. Hartman: "Non-Darcy Measurements in Dry Core and the Effect of Immobile Liquid," paper SPE 39977 presented at the 1998 SPE Gas Technology Symposium, Calgary, Alberta, Canada, March 15-18.
12. Narayanaswamy, G., M. M. Sharma and G. A. Pope: "Effect of Heterogeneity on the Non-Darcy Flow Coefficient," *SPE Res. Eval. & Eng.* (June, 1999) **2**(3), 296-302.
13. Kumar, R.: "Productivity Improvement in Gas Condensate Reservoirs Through Fracturing," MS Thesis, The University of Texas at Austin, August 2000.

Table 1—Experimental Core Properties

Type	Texas Cream limestone
Length (in)	8.0
Diameter (in)	1.0
Porosity (%)	20
Pore Volume (cc)	~20
Brine (%wt $CaCl_2$)	0.5
Water saturation (%)	0-50
Gas Permeability (md)	4-11

Table 2—Composition of Gas Mixture

Component	Mole Fraction
CH4	0.800
n-C4	0.150
n-C7	0.038
n-C10	0.012
Total	1.000

Table 3—Properties of Experimental Gas Mixture at 145°F

Pressure (psig)	Viscosity (cp)
3000	0.0376
2500	0.0246
1200	0.0139

Table 4—Gas Relative Permeability Data After Condensate Accumulation

		Before Methanol Injection				After Methanol Injection		
Exp. No.	P (psig)	Q (cc/hr)	S_o (%)	k_{rg}	N_c (x10^{-5})	Q (cc/hr)	k_{rg}	N_c (x10^{-5})
6	1200	22.4	44	0.029	0.17	-	-	-
7	1000	12.8	45	0.067	0.062	-	-	-
	1200	12.8	44	0.046	0.13	16	0.067	0.076
	1500	12.8	51	0.060	0.11	-	-	-
	2000	12.8	45	0.069	0.24	-	-	-
	2500	12.8	44	0.108	1.2	-	-	-
8	1200	22.4	38	0.027	0.16	16	0.040	0.087
9	2500	12.8	28	0.091	1.4	12.8	0.22	0.43
10	2500	12.8	53	0.073	1.8	12.8	0.076	1.2
11	2500	32	52	0.26	1.1	32	0.17	1.3
12	1200	6.4	8	0.0070	0.31	6.4	0.033	0.064

Table 5—Summary of End-Point Gas Relative Permeability

					Before Methanol Injection				After Methanol Injection		
Exp. No.	P (psig)	k (md)	S_w (%)	Methanol (PV)	S_{or} (%)	Q (cc/hr)	k°_{rg}	N_c (x10^{-5})	Q (cc/hr)	k°_{rg}	N_c (x10^{-5})
6	1200	6.32	10	0	34	32	0.29	0.013	-	-	-
					34	64	0.37	0.032	-	-	-
					34	89.6	0.41	0.039	-	-	-
7	1200	5.14	10	2.0	37	53.9	0.27	0.036	53.9	0.43	0.035
8	1200	4.28	20	5.0	32	53.9	0.22	0.055	53.9	0.34	0.26
9	2500	4.13	20	5.0	8.6	32	0.44	0.76	32	0.62	0.48
10	2500	6.33	0	5.0	51	-	-	-	12.8	0.78	0.35
					51	32	0.55	0.62	32	0.62	1.1
					51	64	0.51	1.3	64	0.60	2.3
					51	89.6	0.50	1.9	-	-	-
11	2500	8.37	0	5.0	22	-	-	-	16	0.75	0.23
					22	32	0.77	0.43	-	-	-
					22	64	0.70	0.96	-	-	-
					22	89.6	0.76	1.2	-	-	-
12	1200	11.29	50	5.0	5	16	0.059	0.023	16	0.17	0.017
					5	32	0.088	0.031	32	0.21	0.028

Table 6—End-Point Gas Relative Permeability Data for Each Section of Core

		Before Methanol Injection					After Methanol Injection				
Exp. No.	S_w (%)	1	2	3	4	Overall	1	2	3	4	Overall
7	10	0.47	0.45	0.26	0.31	0.27	0.71	0.84	0.50	0.58	0.43
8	20	0.42	0.81	0.36	0.21	0.22	0.82	1.00	0.38	0.40	0.34
9	20	0.71	0.62	0.38	0.51	0.44	0.73	0.59	0.50	1.00	0.62
10	0	0.52	0.56	0.47	0.73	0.52	0.95	0.40	0.52	0.50	0.66
11	0	0.82	0.66	0.64	1.00	0.75	-	-	-	-	0.75
12	50	0.24	0.10	0.053	0.052	0.074	0.16	0.27	0.14	0.24	0.19

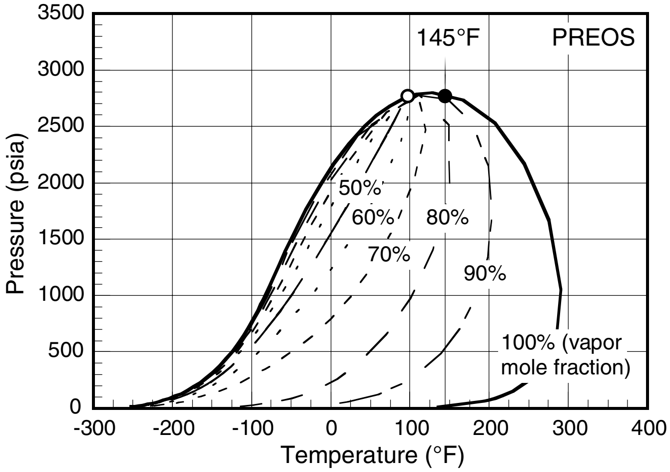

Fig. 1—Phase envelope of gas condensate.

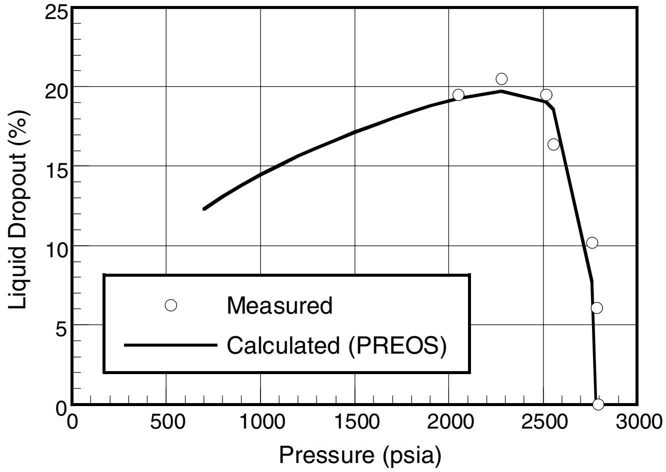

Fig. 2—Liquid dropout for gas condensate at 145°F.

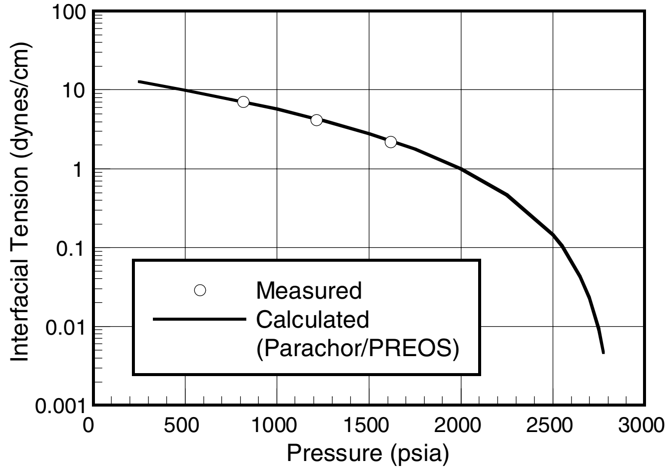

Fig. 3—Interfacial tension for gas condensate at 145°F.

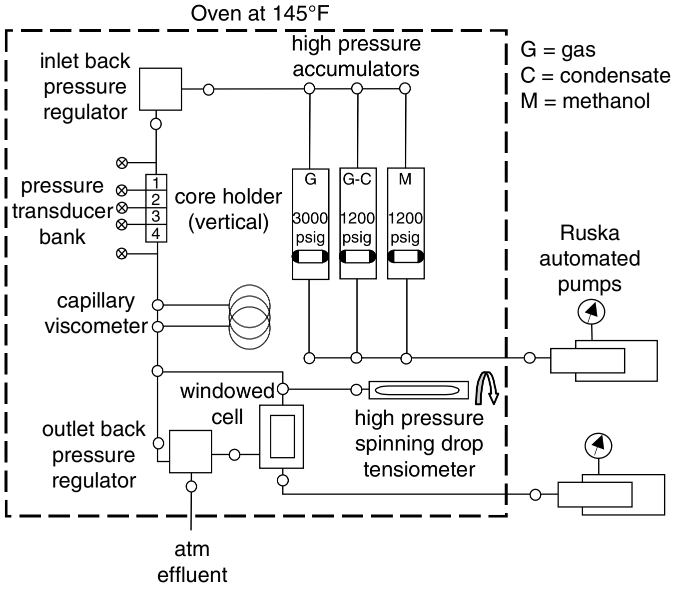

Fig. 4—Gas condensate coreflood apparatus.

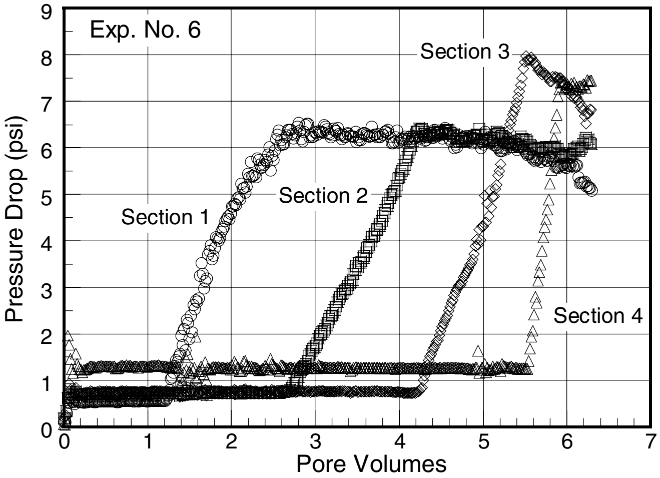

Fig. 5—Pressure drop during condensate accumulation.

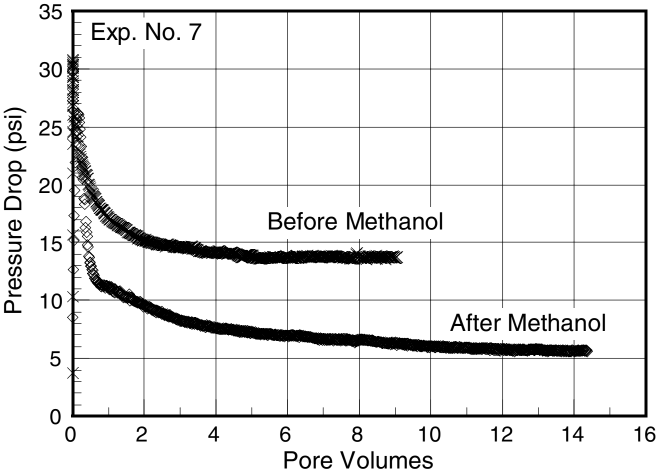

Fig. 6—Overall core pressure drop during gas flood.

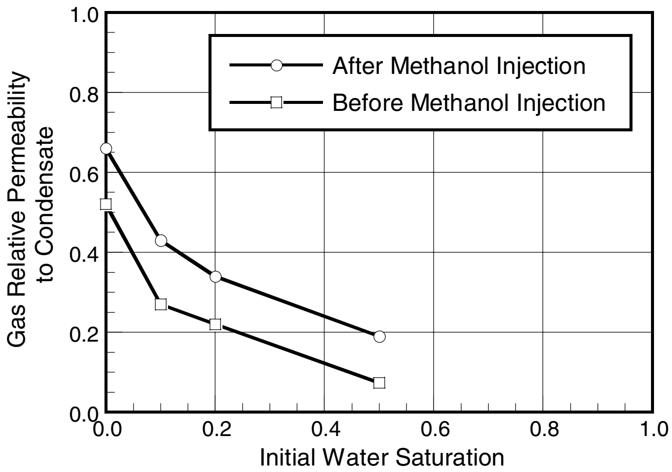

Fig. 7—End-point gas relative permeability before and after methanol injection.

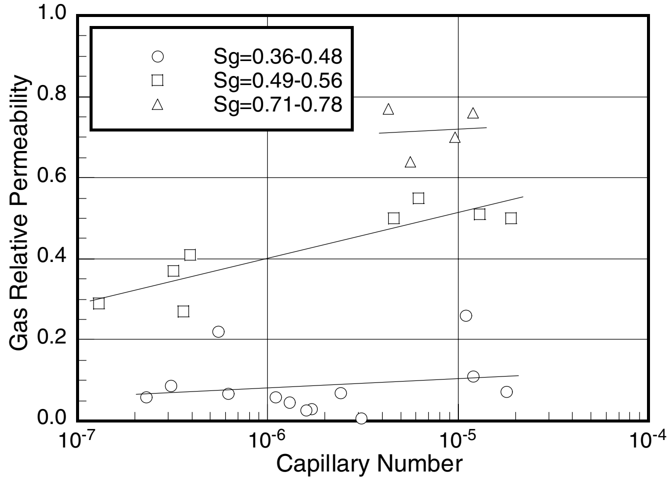

Fig. 8—Gas relative permeability.

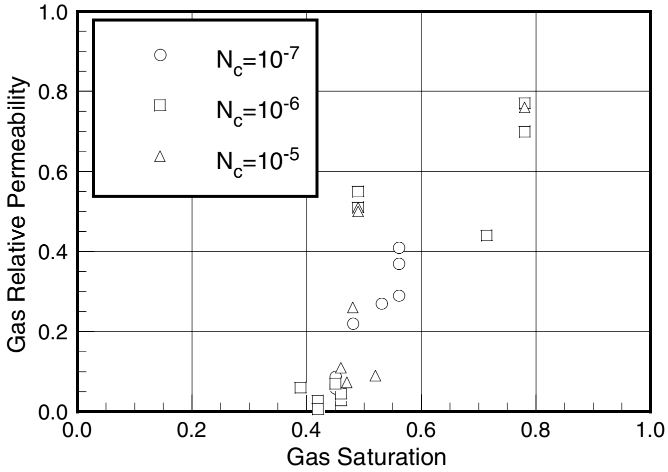

Fig. 9—Gas relative permeability.

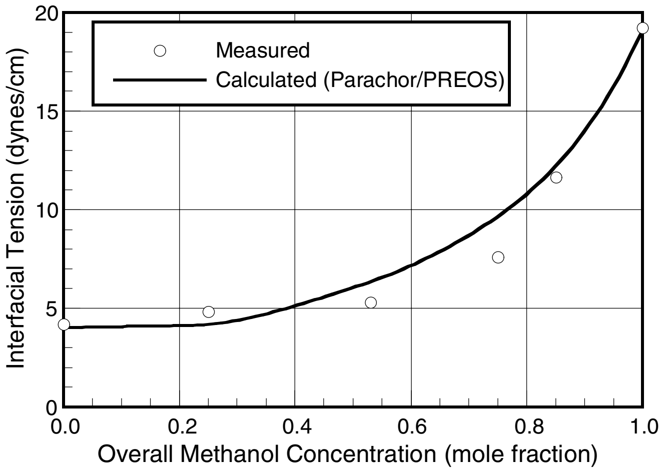

Fig. 10—Interfacial tension between vapor and liquid at bubble point pressure at 145°F.

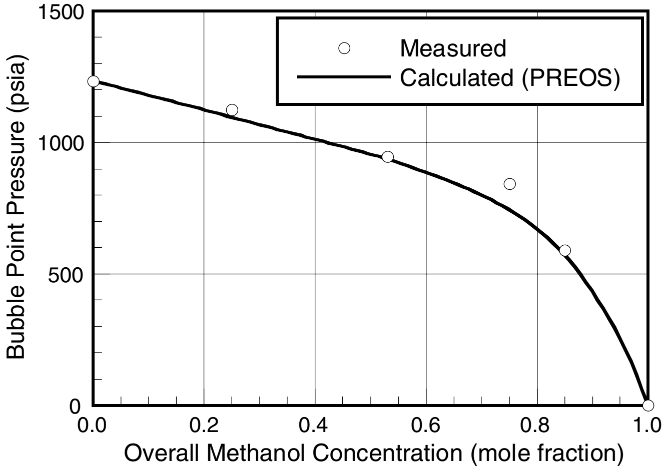

Fig. 11—Effect of methanol on condensate bubble point pressure.

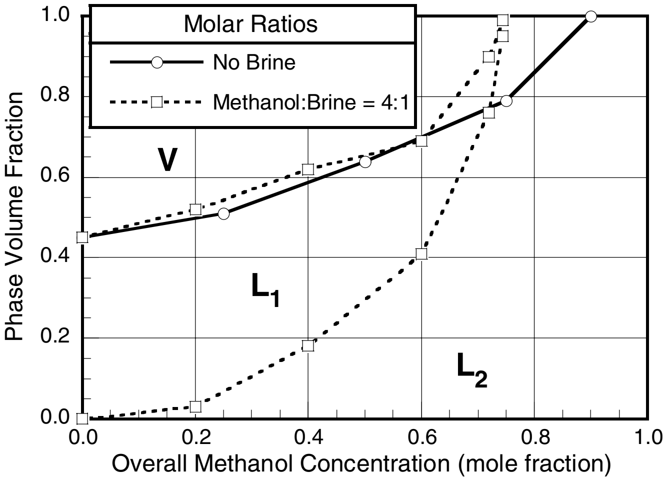

Fig. 12—Phase volume fractions for hydrocarbon-methanol-brine mixtures at 1200 psig and 145°F.